Site seismic response analysis based on vertical borehole records of Chiba

H.P. Ding, J. Liao & Q.J. Ren

Key Laboratory of Structure Engineering of Jiangsu Province, Suzhou University of Science and Technology, Suzhou，China.

Y.Y. Yu

Institute of Engineering Mechanics, China Earthquake Administration, Harbin 150080, China.

ABSTRACT: Many vertical borehole arrays have been built in recent years, and the seismic records at different depth are obtained from them. Using these records, seismic responses of the site can be simulated and represented, which is of great help to the improvement of soil response calculation model and method. In this paper, the conclusion is drawn by theoretical analysis that when the borehole array records are used as the incident waves for soil layer seismic response analysis, the rigid bottom boundary condition should be used. Then by using the vertical borehole array records and borehole profile information of Chiba, Japan, soil seismic response of this region is simulated using the equivalent linear method. By comparison with the real records, the above conclusion is validated. Besides, for the seismic records and borehole profile data used in this paper, the equivalent linear method for soil seismic response analysis has considerable accuracy.

1 INTRODUCTION

The equivalent linear method (Idriss and Seed, 1968) is one of the major tools for the soil seismic response analysis at present. It assures enough accuracy for the calculation results in many conditions, and preserves problems as well, especially when the soil nonlinear effect becomes stronger, the calculation errors also increase accordingly. Li *et al.*(2001) analysed the effect of different site conditions on the ground motions and concluded that when the ground motion is quite strong, calculated results of the sites with soil thickness greater than 50 m and S-wave velocity between 150 - 250 m/s (Ⅲ, Ⅳ category sites according to China code) show obvious discrepancy with real records. Yang *et al.*(2000) calculated the fundamental period of the soft soil site in Nanjing using the equivalent linear method and found that considerable difference exits compared with the fundamental period tested in practice. Qi & Qian(2000) proposed that the equivalent linear method adapted by the nuclear power station aseismic design has many accuracy problems under deep soft soil condition.

  With the development of the strong ground motion observation techniques, under-ground borehole arrays have been installed in many countries. Numerous collocated records recorded at the surface and underground vertical arrays are obtained (Xie *et al.*, 1999; Kurtuluş, 2011; Graizer *et al.*, 2000; Tsai and Lee, 2005). These records provide verification basis for the soil seismic response analysis in theory, method and the reliability of the calculation model. For instance, using these records, the accuracy of the improved equivalent linear method considering the frequency-dependent soil stiffness and damping was examined (Sugito and Masuda, 1994; Furumoto *et al.*, 2002; Yoshida and Suetomi, 1996; Yoshida *et al.*, 2002; Kausel and Assimaki, 2002; Jiang and Xing, 2007).

  When using the vertical borehole array records in soil seismic response calculation, it is important to select an appropriate boundary condition for the soil calculation model. Most of the present soil seismic response analysis methods assume that the base rock is an elastic half space or a rigid basement. This paper first derives the transfer functions corresponding to the two boundary conditions, respectively, and explores which bottom boundary condition should be employed when the real data recorded by the underground strong motion seismograph are directly used as the incident wave in the soil seismic response analysis. Then by the comparison between the calculation results of a real site using the DEEPSOIL program (Hashash *et al.*, 2002) based on equivalent linear method and the field measured data, the reasonability of the conclusion is further verified.

2 BOTTOM BOUNDARY CONDITION WHEN USING BOREHOLE ARRAY RECORDS

The rigid rock basement acts as a fix boundary, so its motions are not affected by the overlying soil, and all the downward travelling waves in the soil will be completely reflected back to the surface when they reach the rigid rock. The elastic basement acts like transmitting boundary, when the downward travelling waves in the soil reach the soil-rock boundary, only part of the energy will be reflected back to the soil, and the other energy will transmit through the boundary and continue to travel in the rock. If the rock extends to great depth, then the energy transmitted through the soil-rock boundary will be completely removed, which is also a form of radiation damping.
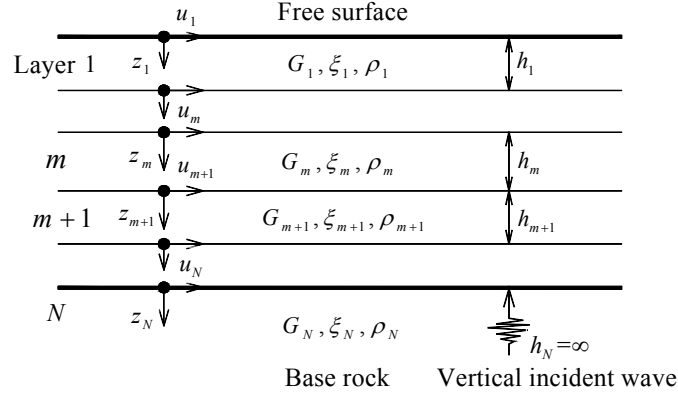

Figure 1 Calculation model of layered soil for seismic response analysis

Consider a layered soil deposits overlying an uniform and isotropic semi-infinite rock basement, and shear waves that propagate vertically from the rock into the overlying soil layers. The calculation model is shown in Figure 1, where the local coordinate system is introduced that assumes that the origins of each layer are located at their tops, respectively, with the positive direction of the Z axis downward. The parameters of each layer and their identifiers(1，…m，　m+1，…N) are also demonstrated in the figure, with notation N indicates the rock, and the G_i, ξ_i, and ρ_i marked in each layer represent the shear modulus, the damping ratio and the mass density, respectively.

Based on one-dimensional shear wave motion theory, the displacement in the soil layers can be expressed as (Kramer, 1996)

$$u(z,t) = Ae^{i(\omega t+k^*z)} + Be^{i(\omega t-k^*z)} \tag{1}$$

where i is the imaginary unit, i.e. $i=\sqrt{-1}$; A and B represent the amplitudes of waves travelling upward (in the -z direction) and downward (in the +z direction), respectively; ω is the circular frequency; k^* indicates the complex wave number that is defined as $k^* = \dfrac{\omega}{v^*} = k(1-i\xi)$ for small ξ.

According to the constitutive relation, the shear stress in each layer is

$$\tau(z,t) = ik^*G(1+2i\xi)(Ae^{ik^*z} - Be^{-ik^*z})e^{i\omega t} \tag{2}$$

Applying the compatibility requirement of displacement and stress to the boundary between layer m and $m+1$, that is

$$u_m(Z_m = h_m, t) = u_{m+1}(Z_{m+1} = 0, t) \tag{3a}$$

$$\tau_m(Z_m = h_m, t) = \tau_{m+1}(Z_{m+1} = 0, t) \tag{3b}$$

Substituting equation (3a) into equation (1) yields

$$A_{m+1} + B_{m+1} = A_m e^{ik_m^* h_m} + B_m e^{-ik_m^* h_m} \tag{4}$$

and substituting equation (3b) into equation (2) yields

$$A_{m+1} - B_{m+1} = \frac{k_m^* G_m^*}{k_{m+1}^* G_{m+1}^*}(A_m e^{ik_m^* h_m} - B_m e^{-ik_m^* h_m}) \tag{5}$$

Adding (4) and (5) and subtracting (5) from (4) gives the recursion formulas of the amplitudes of upward and downward travelling waves, that is,

2

$$A_{m+1} = \frac{1}{2} A_m (1 + \alpha_m^*) e^{ik_m^* h_m} + \frac{1}{2} B_m (1 - \alpha_m^*) e^{-ik_m^* h_m}$$
$$\left.\begin{array}{l} \\ B_{m+1} = \frac{1}{2} A_m (1 - \alpha_m^*) e^{ik_m^* h_m} + \frac{1}{2} B_m (1 + \alpha_m^*) e^{-ik_m^* h_m} \end{array}\right\} \tag{6}$$

where α_m^* is the complex impedance ratio between layer m and layer m+1 that is define as

$$\alpha_m^* = \frac{k_m^* G_m^*}{k_{m+1}^* G_{m+1}^*} = \frac{\rho_m (v_s^*)_m}{\rho_{m+1} (v_s^*)_{m+1}} \tag{7}$$

Rewritten equation (6) in the form of matrix yields

$$\begin{bmatrix} A_{m+1} \\ B_{m+1} \end{bmatrix} = T_m \begin{bmatrix} A_m \\ B_m \end{bmatrix} \tag{8}$$

where T_m is referred as the transfer matrix, and

$$T_m = \begin{bmatrix} \frac{1}{2}(1 + \alpha_m^*) e^{ik_m^* h_m}, \frac{1}{2}(1 - \alpha_m^*) e^{-ik_m^* h_m} \\ \frac{1}{2}(1 - \alpha_m^*) e^{ik_m^* h_m}, \frac{1}{2}(1 + \alpha_m^*) e^{-ik_m^* h_m} \end{bmatrix} \tag{9}$$

Since the shear stress at the free surface (z=0) must be equal to zero, it requires that $A_1=B_1$ from equation (2), and equation (8) becomes

$$\begin{bmatrix} A_N \\ B_N \end{bmatrix} = T_{N-1} \begin{bmatrix} A_{N-1} \\ B_{N-1} \end{bmatrix} = T_{N-1} \cdot T_{N-2} \cdots T_1 \begin{bmatrix} 1 \\ 1 \end{bmatrix} A_1 = T \begin{bmatrix} 1 \\ 1 \end{bmatrix} A_1 = \begin{bmatrix} T_{11} + T_{12} \\ T_{21} + T_{22} \end{bmatrix} A_1 \tag{10}$$

where T is a frequency-dependent function and has the form of complex matrix.

Based on the local coordinate system, the displacements at the ground surface and the top of the rock are

$$u_1(Z_1 = 0, t) = (A_1 + B_1) e^{i\omega t} = 2 A_1 e^{i\omega t} \tag{11}$$
$$u_N(Z_N = 0, t) = (A_N + B_N) e^{i\omega t} \tag{12}$$

Dividing equation (11) by (12), the transfer function corresponding to the rigid rock basement, $F_1(\omega)$, is obtained

$$F_1(\omega) = \frac{2 A_1}{A_N + B_N} = \frac{2}{T_{11} + T_{12} + T_{21} + T_{22}} \tag{13}$$

Dividing equation (11) by the displacement at the outcrop rock, i.e. $2 A_N$, gives the transfer function corresponding to the elastic rock basement, $F_2(\omega)$, that is

$$F_2(\omega) = \frac{2 A_1}{2 A_N} = \frac{1}{T_{11} + T_{12}} \tag{14}$$

At this moment, the frequency domain response of the free surface can be obtained by converting the incident time history into frequency domain, and then multiplying it by the transfer function between the free surface and the top of the layer where incident wave starts. The time domain response can naturally be determined by the inverse Fourier transform.

The above seismic response analysis method for one-dimensional soil is developed with the displacement, but it is also suitable to velocity and acceleration. If the acceleration response needs to be solved, it is just needed to replace the $u(z,t)$ with $a(z,t)$ in the above formulas.

free surface motion

rock outcroping motion

$2A_1$ soil $2A_N$

soil-rock boundary motion
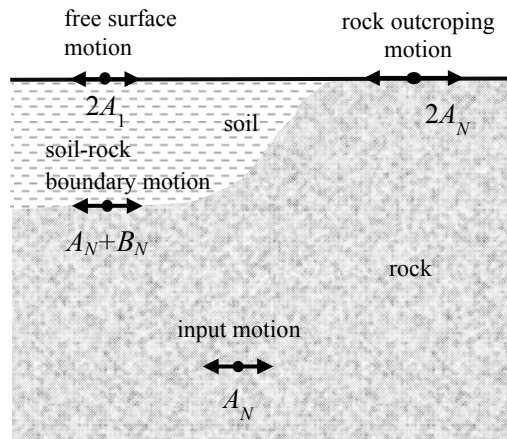
A_N+B_N

rock

input motion

A_N

Figure 2 Simplified sketch of the relationship between seismic motions within the soil

Schematic illustration of the relationship between inner-soil seismic motions is shown in Figure 2. For the vertical borehole array records, the motion at the bottom can be regarded as the seismic motion at the soil- rock boundary, that is, at the top of the rock base. Record at this place already considers the soil-rock interaction that consists of the incident and reflected wave fields, so it is the final response for this point. If this record is used as the incident wave for soil seismic response analysis, the motion should not be changed, subsequently, we need to assume the soil-rock boundary as a rigid base to avoid considering the soil-rock interaction twice.

3 CHIBA SITE AND ITS BOREHOLE ARRAY RECORDS

Chiba site is located at the Industrial Institute of Science, Tokyo University of Japan. The geological section of this site (Furumoto *et al.*, 2002) is presented in Figure 3. The accelerographs are installed in depth of 1m, 5m, 10m, 20m, and 40m beneath the surface. During the 1987 Chiba-ken Toho-oki earthquake (Mw 6.7), the borehole array stations in this site recorded the strong ground motions at different depths. The three component accelerograms at these depths are shown in Figure 4 after baseline correction. In the followings, the GL-1m, GL-5m, GL-10m, GL-20m, and GL-40m denote the positions at depth of 1m, 5m, 10m, 20m, and 40m beneath the surface, respectively.

No.	Depth (m)	Layer thickness (m)	Profile & accelerographs position	Soil number & type	Vs (m/s)	Unit weight (KN/m³)
1	5	5		① loam	140	11. 3
2	10	5		② sandy soil	320	14. 7
3	24	14		③ fine sand	320	19. 1
4	40	16		③ fine sand	420	19. 6
5	—	—		③ fine sand	420	19. 6

Figure 3 Geological profile and observation point positions of the Chiba site
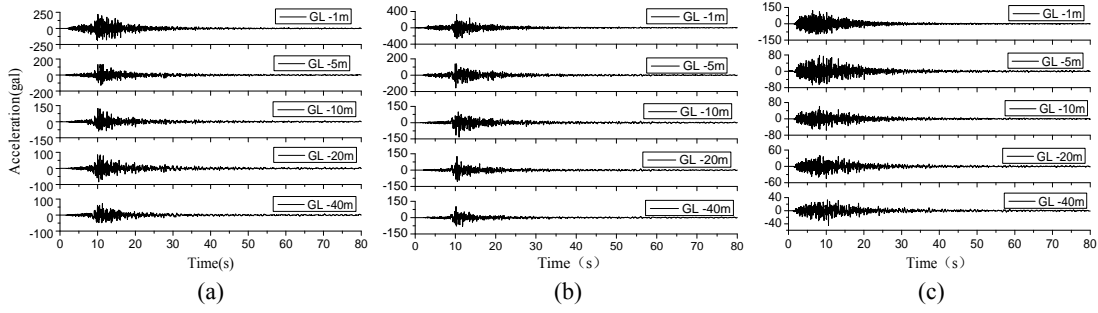
Figure 4 Observed accelerograms at different depth.(a) EW component, (b) NS component, and (c) vertical component,

The soil slice thickness of the calculation model for 1D soil seismic response analysis in Chiba site is determined by

$$h_n \leq \left(\frac{1}{6} \sim \frac{1}{10}\right) T_{\min} v_n \tag{15}$$

where $T_{\min}$ is the shortest period of the input motion with engineering significance (0.04 sec is chosen here), and v_n is the shear wave velocity of soil layer n.

According to Equation (15), the mild-clay stratum (5 m) is divided into 10 sub-layers with thickness of 0.5 m, and the other soil layers are cut with 1 m subdivisions. The overlying soil is divided into 35 slices in total. The soil nonlinear parameters are listed in Table 1, which are estimated from the average results of the classical soil sample experiments in China.

Table 1. Soil nonlinear data of the Chiba site

No.	Soil No.		**Shear Strain** γ （10^{-4}）							
			0.05	0.1	0.5	1	5	10	50	100
1	①	$G/G_{\max}$	0.994	0.988	0.943	0.892	0.622	0.452	0.241	0.136
		λ	0.029	0.037	0.063	0.077	0.106	0.114	0.122	0.123
2	②	$G/G_{\max}$	0.996	0.992	0.962	0.926	0.714	0.555	0.200	0.111
		λ	0.007	0.011	0.031	0.046	0.092	0.109	0.130	0.133
3	③	$G/G_{\max}$	0.980	0.965	0.885	0.805	0.560	0.448	0.220	0.174
		λ	0.005	0.007	0.020	0.035	0.080	0.100	0.120	0.124

4 CALCULATION RESULTS AND COMPARISON WITH OBSERVED RECORDS

In this section, the EW and NS component accelerograms recorded at a depth of 40 m in Chiba site are used as the incident seismic waves at the bottom of the calculation model, respectively. Then the seismic responses of the above soil model are calculated with the DEEPSOIL program that is based on equivalent linear method and rigid bottom boundary. The resulting accelerograms of EW and NS component at the depth of 1m, 5m, 10m, and 20m are obtained and then compared with the observed records.

4.1 Comparisons of accelerograms and amplitudes

Figure 5 shows the comparison between the calculated horizontal acclerograms at different depth with that of the observations. Since the amplitudes before 5 sec and after 30 sec are quite small, and for the clarity of comparison, only the acceleration time histories between 5 and 30 sec are shown. The peak accelerations are compared in Table 2 and Figure 6.

It is shown in Figure 5 that the simulated accelerograms at different depth agree well with the observed records. For the two components, the calculated results of the NS component agree better.

Defining the error $\delta = (|PGA\ observed| - |PGA\ calculated|)/|PGA\ observed|$, it is presented in

Table 2 and Figure 6 that except the 16.2% error for EW component at depth of 1 km and 25.07% error for NS component at depth of 20 m, the other differences between calculated results and

observations are quite unapparent, and the errors are all within the range of 7.5%.
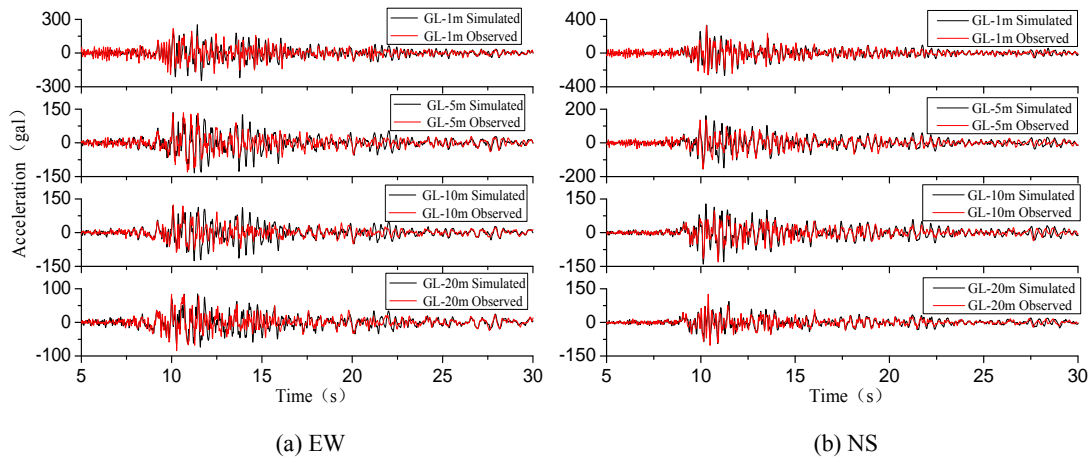

(a) EW

(b) NS

Figure 5 Comparisons between the simulated and observed accelerograms at different depth when the EW and NS component records at a depth of 40m are used as the incident waves

Table 2 Comparisons between the simulated and observed peak accelerations of the Chiba site

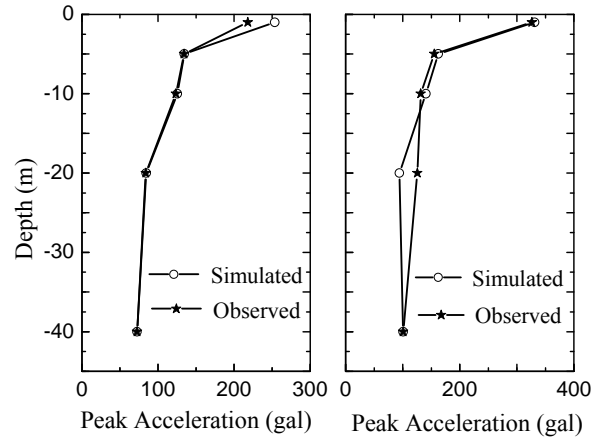| Direction	Depth (m)	Obser. (gal)	Simul. (gal)	Error δ (%)
EW	GL-1m	218.15	253.49	-16.20
	GL-5m	134.23	134.68	-0.33
	GL-10m	123.72	125.66	-1.57
	GL-20m	83.98	84.61	-0.74
NS	GL-1m	326.31	330.96	-1.42
	GL-5m	155.34	162.27	-4.46
	GL-10m	131.51	140.68	-6.97
	GL-20m	125.65	94.15	25.07

Figure 6 Comparisons between the simulated and observed peak accelerations at different depth when the EW and NS component records at a depth of 40m are used as the incident waves

4.2 **Comparisons of the acceleration response spectra**
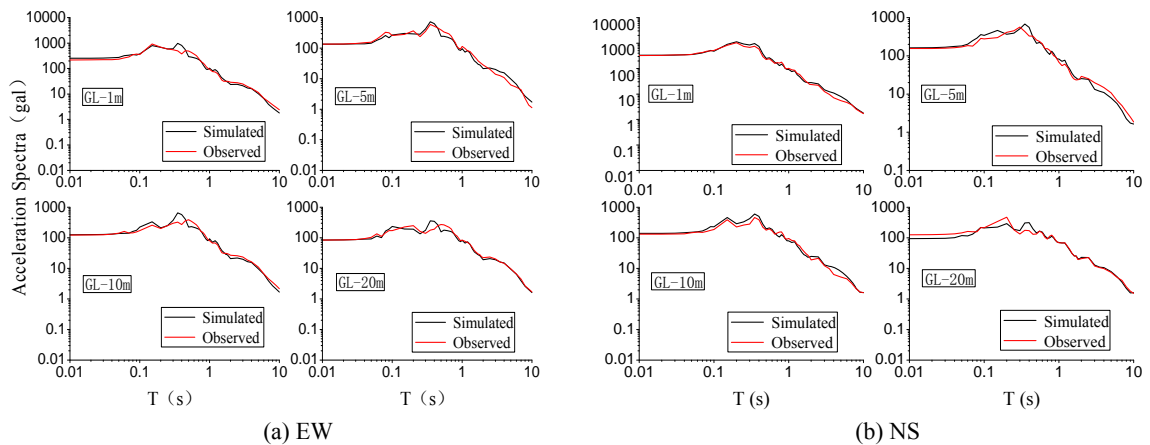

(a) EW

(b) NS

Figure 7 Comparisons between the simulated and observed acceleration response spectrums at different depth when the EW and NS component records at a depth of 40m are used as the incident waves

Acceleration response spectra at different depth are compared in Figure 7. For periods between 0.01 sec and 0.1 sec, the calculated results agree well with the observations except for the EW component at depth of 1 m. In the period range of [0.1, 0.7] sec, the discrepancies between calculations and observations are rather insignificant, however, the difference of the NS component is a little larger. For periods between 0.7 sec and 10 sec, the calculated results agree quite well with the observations.

4.3 **Comparison between the calculated results and the other methods**

Sugito and Masuda (1994) improved the accuracy of the equivalent linear method by considering the frequency-dependent soil shear modulus and damping ratio. Then Yoshida *et al.*(1996;2002) and Kausel & Assimaki (2002) made further development for this method. Jiang and Xing (2007) analysed the previous studies on it and discussed the essence of this method, and a new method considering frequency-dependent parameters was proposed and verified by comparing the calculation results with the observations. Based on the same soil model, we compare our results with the above studies (Fig. 8). It is shown that the results of this paper provide the closest comparisons to the observed data.
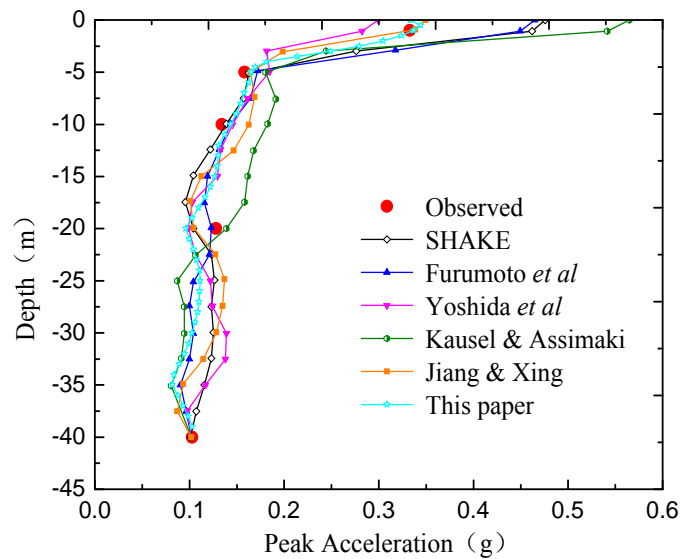

Figure 8 Comparisons of the observed NS component peak accelerations at different depths with the simulation results calculated by different methods

5 **CONCLUSIONS**

The vertical borehole array records are one of the best means of verifying the soil seismic response analysis method and the calculation model. In this paper, the borehole array records of the Chiba site in Japan and its profile are used to perform soil seismic response simulations with the equivalent linear method. By comparing the calculated results with the real records, it is shown that: (1)When the borehole array records are directly used as the incident wave in the soil seismic response analysis, the rigid base should be applied at the bottom boundary; (2) For the seismic records and borehole profiles studied in this paper, the equivalent linear method shows considerable accuracy; (3) A new soil seismic response analysis method can be tested by comparing the calculation results for a site with the records, but appropriate calculation model should be selected first, and then parameter analysis can be made.

In this paper, only the data completed records are used to verify the method we proposed, and further verification and improvement based on rigid bottom boundary should be performed by considering different site conditions and wave amplitudes.

REFERENCES:

Furumoto Y., Sugito M., Yashima A. 2002. Frequency-dependent equivalent linearized technique for FEM response analysis of ground, in 13th WCEE. Auckland, New Zealand.

Graizer V., Shakal A. & Hipley P. 2000. Recent data recorded from downhole geotechnical arrays, in Proceedings of SMIP2000 Seminar on Utilization of Strong-motion Data. California: Sacramentro, 23-38.

Hashash Y.M.A., Groholski D.R., Phillips C. A., *et al*. 2012. DEEPSOIL 5.1, User Manual and Tutorial. 107 p.

Idriss I. M., Seed H. B. 1968. Seismic response of horizontal soil layers. *Journal of the Soil Mechanics and Foundations Division, ASCE*, 94(SM4): 1003-1031.

Jiang T., Xing H. L. 2007. An equivalent linear method considering frequency-dependent soil properties for seismic response analysis. *Chinese Journal of Geotechnical Engineering*, 29(2): 218-224. (in Chinese)

Kausel E. & Assimaki D. 2002. Seismic simulation of inelastic soils via frequency-dependent moduli and damping. *Journal of Engineering Mechanic*s, *ASCE*, 128(1): 34-46.

Kramer, S. L. 1996. Geotechnical earthquake engineering. New Jersey: Upper Saddle River.

Kurtuluş A. 2011. Istanbul geotechnical downhole arrays. *Bulletin of Earthquake Engineering*, 9(5): 1443- 1461.

Li X. J., PENG Q. & Liu W. Z. 2001. Consideration of site effects for determination of design earthquake ground motion parameters. *World Earthquake Engineering*, 17(4): 34-41. (in Chinese)

Qi C. Z., Qian Q. H. 2000. Overview of seismic research for nuclear power plant. *Earthquake Engineering and Engineering Dynamics*, 20(3): 76-86. (in Chinese)

Sugito M. G. H. and Masuda T. 1994. Frequency-dependent equivalent linearized technique for seismic response analysis of multi-layered ground. *Journal of Geotechnical Engineering, JSCE*, 493(III-27): 49–58.

Tsai Y. B., Lee C. P. 2005. Strong motion instrumentation programs in Taiwan, Directions in Strong Motion Instrumentation. Springer: Netherlands, 255-278.

Xie L. L., Li S. B., Zhang W. B. 1999. A three dimensional array for site effects on strong ground motion. *Earthquake Engineering and Engineering Dynamics*, 19(2): 1-8. (in Chinese)

Yang W. L., Chen G. X., *et al*. 2000. Study of influence of deep level excavation on design ground motion parameters in a weak foundation site. *Earthquake Engineering and Engineering Dynamics*, 20(3)：93-99. (in Chinese)

Yoshida N., Kobayashi S., Suetomi I., *et al*. 2002. Equivalent linear method considering frequency dependent characteristics of stiffness and damping. *Soil Dynamics and Earthquake Engineering*, 22(3): 205-222.

Yoshida N, Suetomi I. 1996. DYNEQ: a computer program for dynamic analysis of level ground based on equivalent linear method. Reports of Engineering Research Institute, Sato Kogyo Co. Ltd, 61-70.